Solubility of 1-Alkyl-3-methylimidazolium Hexafluorophosphate in Hydrocarbons†

Urszula Domańska* and Andrzej Marciniak

Warsaw University of Technology, Faculty of Chemistry, Physical Chemistry Division, Noakowskiego 3, 00-664 Warsaw, Poland

The solubilities of 1-ethyl-3-methylimidazolium hexafluorophosphate, [emim][PF_6], in aromatic hydrocarbons (benzene, toluene, ethylbenzene, *o*-xylene, *m*-xylene, *p*-xylene) and of 1-butyl-3-methylimidazolium hexafluorophosphate, [bmim][PF_6], in the same aromatic hydrocarbons, in *n*-alkanes (pentane, hexane, heptane, octane), and in cyclohydrocarbons (cyclopentane, cyclohexane) have been measured by a dynamic method from 290 K to the melting point of the ionic liquid or to the boiling point of the solvent. The melting point, enthalpy of fusion, and enthalpies of solid−solid phase transitions were determined by differential scanning calorimetry (DSC). The solubilities of [emim][PF_6] and [bmim][PF_6] in aromatic hydrocarbons decrease with an increase of the molecular weight of the solvent. The differences of the solubilities in *o*-, *m*-, and *p*-xylene are not significant. The intermolecular solute−solvent interactions are very small. The liquidus curves were correlated by means of the UNIQUAC and NRTL equations, utilizing parameters derived from the solid−liquid equilibrium. The average root-mean-square deviation of the solubility temperatures for all solvents was 0.41 K and depended on the particular equation used.

Introduction

This paper follows the measurements on a new generation of solvents for catalysis and synthesis—room-temperature ionic liquids (ILs), which have been demonstrated as potential successful replacements for conventional media in chemical processes.[1] They are generally salts based on a substituted imidazolium or pyridinium cation and an inorganic anion such as halide, $[AlCl_4]^-$, or $[BF_4]^-$ or $[PF_6]^-$, and they are often liquids at room temperature. Room-temperature ionic liquids are being investigated as more clean replacements for volatile organic solvents. The important properties include high heat capacity, high density, high thermal conductivity, extremely low volatility, nonflammability, high thermal stability, wide temperature range for the liquid phase, many variations in compositions, and large number of possible variations in cation and anion conformation, allowing fine-tuning of the ionic liquid properties for specific applications. A major reason for the interest in ILs is their negligible vapor pressure, which decreases the risk of technological exposure and the loss of solvent to the atmosphere. A review of recent applications of ILs has been presented along with some results of measurements of liquid−liquid equilibria and partition coefficients with alcohols.[2]

Qualitative and quantitative vapor−liquid equilibrium and liquid−liquid phase behavior of water and three ionic liquids—1-butyl-3-methylimidazolium hexafluorophosphate, [bmim][PF_6], 1-octyl-3-methylimidazolium hexafluorophosphate, [C_8mim][PF_6], and 1-octyl-3-methylimidazolium tetrafluoroborate, [C_8mim][BF_4]—has been reported.[3] The solubilities of water in the liquids [emim][PF_6] and [bmim][BF_4] as a function of temperature have also been reported.[4] The complete understanding of the phase behavior of ILs with water is an important issue. The presence of water in the IL phase can dramatically affect the physical properties.[2] ILs form glasses at low temperatures and have minimal vapor pressure up to their thermal decomposition temperature, which was determined for [emim][PF_6] as 648.15 K.[5] The solvent strength and polarity of some imidazolium ([bmim][PF_6] and [C_8mim][PF_6]) ionic liquids, as measured using two different fluorescent probes, indicated that these liquids were more polar than acetonitrile but less polar than methanol.[6] The surface tension of [bmim][PF_6] is high (47 mJ/m^2), close to that of imidazole, while the surface tensions of the longer-chain [PF_6] homologes are lower and approach those of an alkane.[7] To design any process involving ionic liquids on an industrial scale, it is necessary to know a range of physical properties, including viscosity, density, interfacial tension, and heat capacity, as well as liquid−liquid equilibrium and solid−liquid equilibrium data.

The densities, surface tensions, octanol/water partition coefficients for some imidazoles[8,9] and ionic liquids,[10] and solid−liquid equilibria or liquid−liquid equilibria for imidazole[11−13] and ionic liquids[10,14] in binary mixtures were investigated.

The purpose of this paper was to report the solubilities of 1-ethyl-3-methylimidazolium hexafluorophosphate, [emim][PF_6], in aromatic hydrocarbons (benzene, toluene, ethylbenzene, *o*-xylene, *m*-xylene, *p*-xylene) and of 1-butyl-3-methylimidazolium hexafluorophosphate, [bmim][PF_6], in the same aromatic hydrocarbons, in *n*-alkanes (pentane, hexane, heptane, octane), and in cyclohydrocarbons (cyclopentane, cyclohexane). This work also leads to a better understanding of the specific interaction between the nitrogen atoms of the IL molecule and the aromatic ring of the alkyl-substituted benzenes.

Experimental Section

The origins of the chemicals (in parentheses Chemical Abstract registry numbers, the manufactures reported, and

† This contribution will be part of a special print edition containing papers presented at the Workshop on Ionic Liquids at the 17th IUPAC Conference on Chemical Thermodynamics, Rostock, Germany, July 28 to August 2, 2002.

* Corresponding author. E-mail: ula@ch.pw.edu.pl.

10.1021/je020145g CCC: $25.00
Published on Web 02/27/2003

mass percent purities) were as follows: [emim][PF_6] (155371-19-0, Solvent Innovation GmbH, ≥98%); [bmim][PF_6] (174501-64-5, Solvent Innovation GmbH, ≥98%); benzene (71-43-2, Aldrich, 99.97+%); toluene (108-88-3, POCh, Poland for analysis); ethylbenzene (100-41-4, Aldrich, 99%); *o*-xylene (95-47-6, Fluka, ≥99%); *m*-xylene (108-38-3, Fluka, ≥99%); *p*-xylene (106-42-3, Aldrich, 99%); cyclopentane (287-92-3, Merck, 98%); cyclohexane (110-82-7, Intern. Enz. Lim., for spectroscopy); pentane (110-66-0, Fluka, purum); hexane (110-54-3, Merck, 99%); heptane (142-82-5, Aldrich, 99%); octane (111-65-9, Aldrich, 99%). The substances [emim][PF_6] and [bmim][PF_6] were used without further purification. The purity of the [bmim][PF_6] sample was determined to be 99.2 mol % by fractional melting. The other solvents were fractionally distilled over different drying reagents to a mass fraction purity better than 99.8 mass %, determined by GLC. Liquids were stored over freshly activated molecular sieves of type 4 Å (Union Carbide).

Procedures. Molar enthalpies of fusion and solid−solid phase transitions have been measured with the differential scanning microcalorimeter Perkin-Elmer Pyris 1. Measurements of the fusion enthalpies were carried out at a scan rate of 10 K·min^{-1}, a power sensitivity of 16 mJ·s^{-1}, and a recorder sensitivity of 5 mV. The instrument was calibrated against a 99.9999 mol % purity indium sample. The calorimetric accuracy was ±1%, and the calorimetric precision was ±0.5%.

Solid−liquid equilibrium (SLE) and liquid−liquid equilibrium (LLE) temperatures were determined using a dynamic method described in detail previously.[11] Appropriate mixtures of solute and solvent placed under the nitrogen in drybox into a Pyrex glass cell were heated very slowly (less than 2 K·h^{-1} near the equilibrium temperature) with continuous stirring inside a cell which was placed in a glass thermostat filled with silicone oil, or water, or with acetone and dry ice. The liquid of the bath was changed for the certain range of the temperature measured. The temperature at which the last crystals disappeared was taken as the temperature of the (solid + liquid) equilibrium in the saturated solution. The crystal disappearance temperatures were detected visually. The disappearance of the cloud in the middle of the liquid phase in LLE observed with increasing temperature was also detected visually. The temperature was measured with an electronic thermometer P 550 (DOSTMANN electronic GmbH) with the probe totally immersed in the thermostating liquid. The thermometer was calibrated on the basis of ITS-90. The accuracy of the temperature measurements was judged to be ±0.01 K. Mixtures were prepared by mass, and the errors did not exceed $\delta_{x1} = 0.0002$ and $\delta_{T1}/K = 0.1$ in the mole fraction and temperature, respectively. It was found that the solution-crystallization procedure was quite slow and difficult; thus, the solubility measurements were very time-consuming. The LLE measurements were limited at the upper temperature by the boiling point of the solvent.

Results and Discussion

Table 1 and Figure 1 show the pure component DSC results. A search of the literature has indicated that the data for [emim][PF_6] and [bmim][PF_6] presented here have not been published previously. The results of the DSC examination of [bmim][PF_6] were discussed nowadays[20] as a summary effect of melting and transition, and the enthalpy presented was 19.60 kJ·mol^{-1}; the heat capacity jumps were 44.8 J·K^{-1}·mol^{-1} at fusion and 81.6 J·K^{-1}·mol^{-1} at the glass transition.[20] The effects are smaller than typical values for molecular liquids of molecular mass close to that of [bmim][PF_6]. The summary effect for melting and solid−solid phase transition in our results was 19.88 kJ·mol^{-1}. From the thermograph of the pure solute [bmim][PF_6], a phase (α_1) in the region from 276.43 K to 257.95 K with the enthalpy of melting equal to 9.21 kJ·mol^{-1} exists. On the other hand, the transition of [bmim][PF_6] phase α_1 into phase β_1 is accompanied by the higher enthalpy equal to 10.67 kJ·mol^{-1}(ΔH_{trI}). The effect of cool crystallization is also observed in the range of temperatures 257 K to 233 K (see Figure 1b). For simple imidazoles, only 2-methyl-1*H*-imidazole has shown a solid−solid phase transition with the enthalpy of the transition lower than that of fusion.[8] For [bmim][PF_6] a glass transition was observed for temperatures lower than 196.5 K. The half C_p extrapolated was at the temperature 196.5 K with the heat capacity jumps equal to 52.85 J·K^{-1}·mol^{-1}. The influence of water on the DSC data was discussed previously.[2] Our

Table 1. Physical Constants of Pure Imidazolium Salts: T_m, Melting Point; ΔH_m, Enthalpy of Fusion; T_{tr}, Temperature of Solid−Solid Phase Transition (I or II); ΔH_{tr}, Enthalpies of Phase Transitions; ΔC_p, Heat Capacity of the Liquid Phase as Determined from the DSC Measurements; $V^{298.15}$, Molar Volume

	T_m	ΔH_m	T_{trI}/T_{trII}	ΔH_{trI}	V(298.15)
salt	K	kJ·mol^{-1}	K	kJ·mol^{-1}	cm^3·mol^{-1}
[emim][PF_6]	332.80[a]	17.86			242.6[b]
[bmim][PF_6][c]	276.43[d]	9.21	257.95/ 196.56 (glass)	10.67	204.1[e]

[a] The melting point of [emim][PF_6] was reported to be 331−333 K in refs 15 and 16 or 335.15 K in ref 5. [b] Calculated by the group contribution method from ref 17. [c] ΔC_p at the glass transition is equal to 52.85 J·K^{-1}·mol^{-1} (our result). T_{trI}/T_{trII} in kelvin = 257.95/196.56 (glass). [d] The melting point of [bmim][PF_6] was reported to be 277.15 K in ref 16. [e] Calculated from the density, ρ = 1.392 g·cm^{-3} (298.15 K), from ref 18; the other density reported by ref 19, ρ = 1.31 g·cm^{-3} (298.15 K), was neglegted.

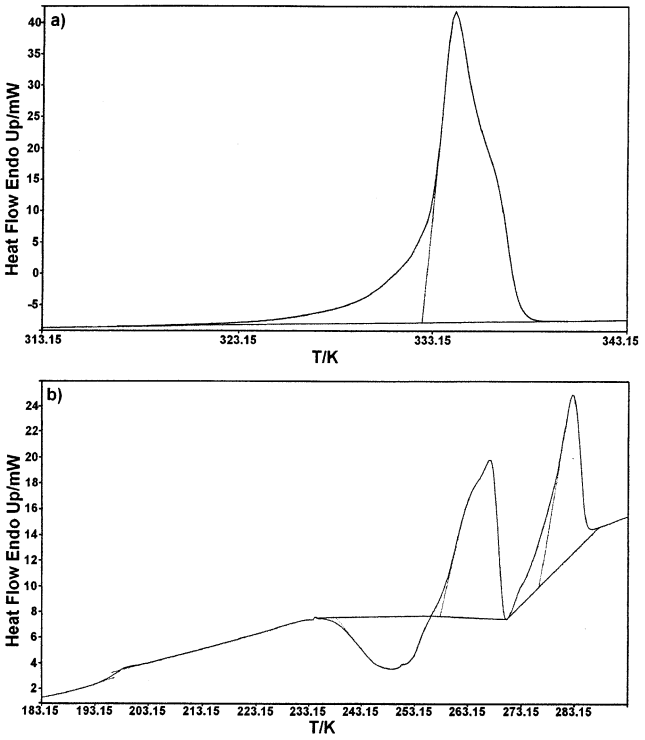

Figure 1. DSC at the scan rate 10 K·min^{-1}: (a) [emim][PF_6]; (b) [bmim][PF_6].

Table 2. Experimental Solid−Liquid Equilibrium Temperatures for {x_1[emim][PF_6] + (1 − x_1)Hydrocarbon} Systems

x_1	T/K	x_1	T/K	x_1	T/K
		Benzene			
0.0152	308.1	0.3382	307.9	0.5201	311.0
0.0360	308.1	0.3680	308.1	0.5499	312.6
0.0523	308.1	0.3907	307.9	0.5767	313.8
0.0895	308.1	0.4154	308.2	0.5810	314.0
0.1198	308.1	0.4307	308.5	0.6250	316.8
0.1514	307.9	0.4337	308.5	0.6739	319.2
0.1836	307.9	0.4456	308.5	0.7408	322.3
0.2135	307.9	0.4500	308.5	0.8041	325.4
0.2435	308.0	0.4686	308.9	0.8639	328.2
0.2754	307.8	0.4687	309.1	0.9478	331.6
0.2859	308.0	0.4945	310.0	1.0000	332.8
0.3194	308.0	0.5183	311.2		
		Toluene			
0.0073	320.8	0.6192	320.8	0.7486	323.3
0.0154	320.8	0.6340	320.8	0.7843	324.5
0.0461	320.9	0.6529	320.9	0.7881	324.6
0.1200	320.9	0.6548	321.0	0.8426	327.6
0.2080	320.8	0.6788	321.1	0.8889	329.4
0.3328	320.8	0.6880	321.1	0.9531	332.1
0.4705	320.8	0.6924	321.1	1.0000	332.8
0.5559	320.8	0.7131	321.6		
0.5990	320.8	0.7250	322.3		
		Ethylbenzene			
0.0071	328.3	0.4825	328.3	0.8128	328.3
0.0150	328.3	0.5648	328.4	0.8423	328.4
0.0760	328.3	0.6354	328.4	0.8723	328.4
0.1564	328.3	0.6879	328.4	0.8999	329.2
0.2154	328.4	0.7043	328.4	0.9325	330.3
0.2745	328.3	0.7352	328.4	0.9675	331.5
0.3489	328.4	0.7604	328.4	1.0000	332.8
0.4132	328.4	0.7833	328.4		
		o-Xylene			
0.0075	325.9	0.6541	326.0	0.8473	326.1
0.0151	325.9	0.6975	326.0	0.8654	326.8
0.0561	326.0	0.7181	326.0	0.8858	328.2
0.1241	325.9	0.7401	326.0	0.9030	328.9
0.1823	326.0	0.7623	326.0	0.9068	328.9
0.2564	325.9	0.7700	326.0	0.9108	329.0
0.3321	325.9	0.7992	326.0	0.9386	330.6
0.4387	325.9	0.8024	326.0	0.9614	331.3
0.5013	326.0	0.8133	326.0	0.9743	331.9
0.5687	326.0	0.8357	326.1	1.0000	332.8
		m-Xylene			
0.0069	327.5	0.6548	327.5	0.8799	328.9
0.0131	327.5	0.7235	327.5	0.8958	329.4
0.0564	327.5	0.7571	327.5	0.9195	330.1
0.1154	327.5	0.7902	327.5	0.9277	330.6
0.1985	327.5	0.7939	327.5	0.9453	331.5
0.2763	327.5	0.8106	327.5	0.9525	331.9
0.3614	327.5	0.8277	327.6	0.9684	332.4
0.4432	327.5	0.8367	327.8	1.0000	332.8
0.5024	327.5	0.8480	328.1		
0.5894	327.5	0.8667	328.3		
		p-Xylene			
0.0075	326.9	0.6542	326.9	0.8521	327.1
0.0183	326.9	0.6784	326.9	0.8660	328.1
0.1024	326.9	0.7270	327.0	0.8856	329.2
0.1752	326.9	0.7588	326.9	0.9173	329.9
0.2536	326.9	0.7774	326.9	0.9272	330.8
0.3374	326.9	0.7958	327.0	0.9488	331.3
0.4102	326.9	0.8080	327.0	1.0000	332.8
0.4985	326.9	0.8174	327.0		
0.5845	326.9	0.8367	327.0		

LLE measurements were made in the liquid phase; thus, we did not observed that effect.

The solubilities of [emim][PF_6] and [bmim][PF_6] in hydrocarbons are shown in Tables 2−4 and in Figures 2−5. The tables include the direct experimental results of the SLE temperatures, T (stable crystalline form), or LLE temperatures versus x_1, the mole fraction of the [e- or bmim][PF_6] in the saturated solution for the investigated systems. The ability of a solute to form hydrogen bonds or other possible interactions with potential solvents is an important feature of its behavior. Basic [emim][PF_6] and [bmim][PF_6] ionic liquids can act both as hydrogen-bond acceptor ([PF_6]$^-$) and donor ([e- or bmim]$^+$) and would be expected to interact with solvents which have both accepting and donating sites. On the other hand, aromatic hydrocarbons are known to form n−π interactions with many solutes.

Table 3. Experimental Liquid−Liquid Equilibrium Temperatures for {x_1[emim][PF_6] + (1 − x_1)Hydrocarbon} Systems

x_1	T/K	x_1	T/K
	Benzene		
0.4307	348.1	0.4456	336.0
0.4337	344.6	0.4500	327.0
	Toluene		
0.5990	378.1	0.6548	351.1
0.6192	367.6	0.6788	337.1
0.6340	361.3	0.6880	327.0
0.6529	351.5		
	Ethylbenzene		
0.7043	405.6	0.7833	372.6
0.7352	396.1	0.8128	354.9
0.7604	387.1	0.8423	332.9
	o-Xylene		
0.6975	413.6	0.7992	352.2
0.7181	401.5	0.8024	350.3
0.7401	388.3	0.8133	345.0
0.7623	376.1	0.8357	332.7
0.7700	371.6	0.8473	327.4
	m-Xylene		
0.7571	394.7	0.8106	360.0
0.7902	371.1	0.8277	346.1
0.7939	369.1		
	p-Xylene		
0.7270	398.3	0.8080	351.7
0.7588	378.8	0.8174	344.1
0.7774	367.1	0.8367	330.6
0.7958	358.1		

Experimental phase diagrams of SLE and LLE investigated in this work are characterized mainly by the following: (1) the mutual solubility of [emim][PF_6] and [bmim][PF_6] in benzene and its alkyl derivatives decreases with an increase of the alkyl substituent at the benzene ring; (2) the liquidus curves exhibit similar shapes; the differences in solubilities are small; the mutual liquid−liquid solubility increases in the order benzene > toluene > ethylbenzene (see Figure 2); (3) positive deviations from ideality were found; thus, the solubility is lower than the ideal one (see dashed line in Figure 2); the activity coefficient of the solute in the saturated solution is higher than 1 ($\gamma_1 > 1$); the one in the one liquid-phase region is in the range from $\gamma_1 = 1.0$ to $\gamma_1 = 1.3$ in different solvents; and the one in the binary liquid-phase region is in the range from $\gamma_1 = 1.4$ to $\gamma_1 = 40$ (benzene), or even to $\gamma_1 = 107$ (toluene); (4) the mutual liquid−liquid solubility of [emim][PF_6] in *o*-xylene and *p*-xylene is comparable and higher than that in *m*-xylene; (5) the shape of the equilibrium curve is similar for [bmim][PF_6] in every *n*-alkane; the temperature of the miscibility gap increases with an increase of the length of the hydrocarbon's alkyl chain (see Figure 3); (6) for cyclohydrocarbons the area of the binary liquids seems to be more flat than that for *n*-hydrocarbons (see Figure 4); (7) the [bmim][PF_6] is more soluble in aromatic compounds than [emim][PF_6] (see Figures 2 and 5); (8) the mutual liquid−liquid solubility of [bmim][PF_6]

Table 4. Experimental Liquid−Liquid Equilibrium Temperatures for {x_1[bmim][PF_6] + (1 − x_1)Hydrocarbon} Systems

x_1	T/K	x_1	T/K
	Benzene		
0.3411	353.2		
0.3471	293.1		
	Toluene		
0.5639	383.7		
0.5680	293.1		
	Ethylbenzene		
0.6548	401.1	0.7220	330.5
0.6768	385.1	0.7294	319.6
0.6945	368.1	0.7359	311.5
0.7070	355.1	0.7459	294.1
0.7127	343.4		
	o-Xylene		
0.6441	401.1	0.6985	353.1
0.6569	385.1	0.7167	329.5
0.6638	382.0	0.7400	293.1
0.6780	366.9		
	m-Xylene		
0.6937	391.1	0.7172	348.6
0.7000	380.7	0.7253	325.1
0.7065	369.1	0.7325	294.1
0.7078	366.1		
	p-Xylene		
0.6905	393.1	0.7253	334.1
0.7007	381.1	0.7386	297.1
0.7134	358.1		
	Pentane		
0.8595	308.7	0.9200	298.6
0.8778	305.7	0.9477	293.5
0.8979	302.7		
	Hexane		
0.8467	342.0	0.9236	322.5
0.8679	337.3	0.9416	314.4
0.8937	329.9		
	Heptane		
0.8714	371.1	0.9415	351.8
0.8919	367.7	0.9551	341.0
0.9255	359.5		
	Octane		
0.8818	394.2	0.9439	366.0
0.9110	383.7	0.9587	357.5
0.9326	371.8	0.9740	347.5
	Cyclopentane		
0.7974	322.8	0.9002	304.3
0.8141	320.0	0.9326	297.1
0.8356	314.8	0.9633	293.1
0.8679	310.1		
	Cyclohexane		
0.7605	352.7	0.8407	337.2
0.7769	350.1	0.8913	325.4
0.8068	345.1	0.9471	302.1

in *m*-xylene and *p*-xylene is comparable and smaller than that in *o*-xylene.

Solid−Liquid Equilibria Correlation

The solubility of a solid compound (1) in a liquid solvent (2) may be expressed as follows:

$$-\ln x_1 = \frac{\Delta H_{m1}}{R}\left(\frac{1}{T} - \frac{1}{T_{m1}}\right) - \frac{\Delta C_{p,m1}}{R}\left(\ln \frac{T}{T_{m1}} + \frac{T_{m1}}{T} - 1\right) + \ln \gamma_1 \quad (1)$$

where x_1, γ_1, ΔH_{m1}, $\Delta C_{p,m1}$, T_{m1}, and T stand for mole fraction, activity coefficient, enthalpy of fusion, difference in solute heat capacity between the solid and the liquid at the melting point, melting point of the solute (compound 1), and equilibrium temperature, respectively. Because of the lack of appropriate data representing the $\Delta C_{p,m1}$ for the systems under investigation, the simplified version of the solubility equation (eq 1) without the $\Delta C_{p,m1}$ term was applied.

In this study two methods are used to correlate the solute activity coefficients, γ_1. They are based on the UNIQUAC [21] and NRTL[22] models describing the excess Gibbs energy. The exact mathematical formulation of these models was given previously.[23]

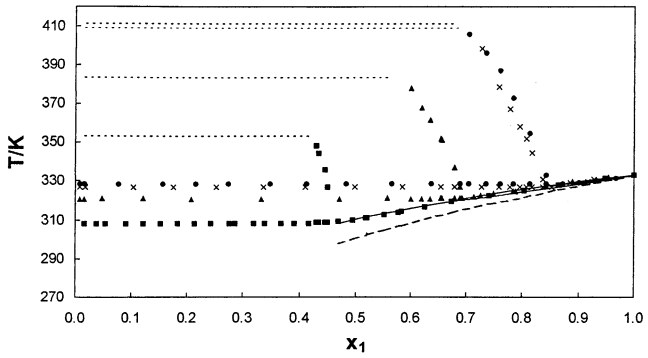

Figure 2. Solid−liquid and liquid−liquid equilibrium diagrams for {x_1[emim][PF_6] + (1 − x_1)aromatic compound}: ■, benzene; ▲, toluene; ●, ethylbenzene; ×, *p*-xylene; solid line, calculated by the NRTL equation; dashed line, ideal solubility; dotted line, boiling temperature of a solvent.

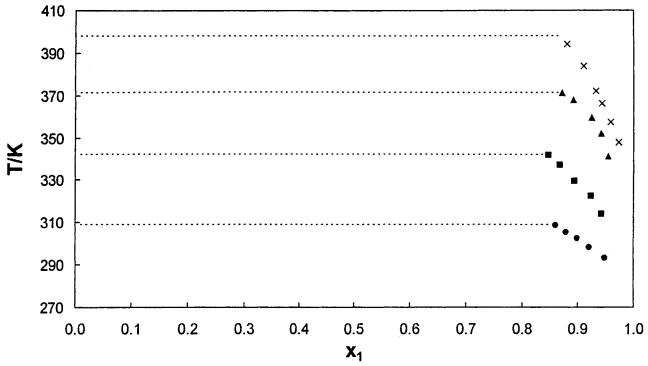

Figure 3. Liquid−liquid equilibrium diagrams for {x_1[bmim][PF_6] + (1 − x_1)*n*-alkane}: ●, pentane; ■, hexane; ▲, heptane; ×, octane; dotted line, boiling temperature of a solvent.

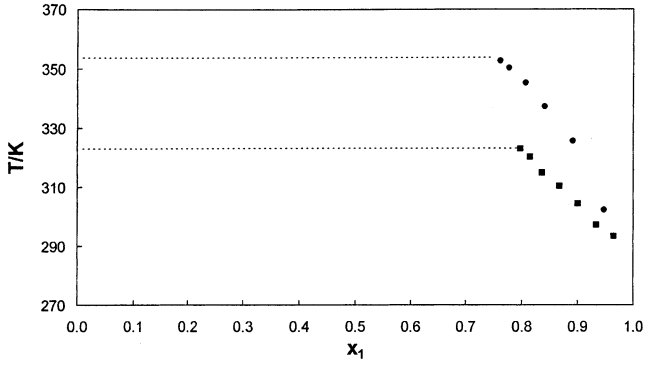

Figure 4. Liquid−liquid equilibrium diagrams for {x_1[bmim][PF_6] + (1 − x_1)cycloalkane}: ■, cyclopentane; ●, cyclohexane; dotted line, boiling temperature of a solvent.

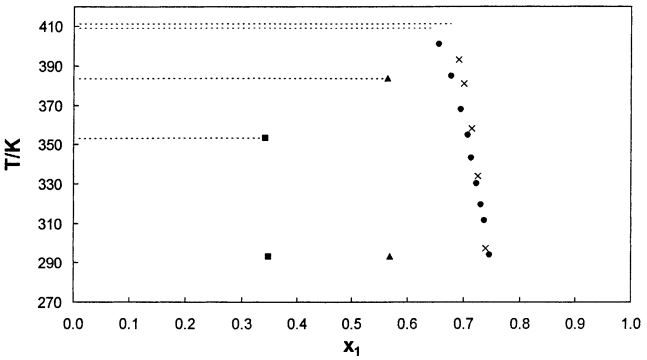

Figure 5. Liquid−liquid equilibrium diagrams for {x_1[bmim][PF_6] + (1 − x_1)aromatic compound}: ■, benzene; ▲, toluene; ●, ethylbenzene; ×, *p*-xylene; dotted line, boiling temperature of a solvent.

Model parameters were found by minimization of the objective function Ω:

$$\Omega = \sum_{i=1}^{n} [T_i^{\exp} - T_i^{\mathrm{cal}}(x_{1i}, P_1, P_2)]^2 \qquad (2)$$

where n is the number of experimental points and $T_i^{\exp}$ and T_i^{cal} denote respectively the experimental and calculated equilibrium temperatures corresponding to the concentration x_{1i}. P_1 and P_2 are model parameters resulting from the minimization procedure. The root-mean-square deviation of temperature was defined as follows:

$$\sigma_T = \left(\sum_{i=1}^{n} \frac{(T_i^{\exp} - T_i^{\mathrm{cal}})^2}{n-2} \right)^{1/2} \qquad (3)$$

The parameters r_i and q_i of the UNIQUAC and NRTL models were calculated with the following relationships:[24, 25]

$$r_i = 0.029281 V_{\mathrm{m}} \qquad (4)$$

$$q_i = \frac{(Z-2) r_i}{Z} + \frac{2(1-l_i)}{Z} \qquad (5)$$

where V_{m} is the molar volume of pure component i at 298.15 K. The coordination number Z was assumed to be equal to 10, and the bulk factor l_i was assumed to be equal to 1. Values of model parameters obtained by fitting solubility curves are given in Table 5 together with corresponding standard deviations.

The results obtained with solubility data of ILs described by two models are similar. The best representation of the liquidus curve in binary phases of [emim][PF_6] in aromatic hydrocarbons was obtained using the NRTL equation with the resulting standard deviation $\sigma_T = 0.40$ K.

Conclusions

The liquid−liquid phase diagrams for the mixtures under study exhibited upper critical solution temperatures (USCTs). The area of two liquid phases decreases with an increase in the chain length of the alkyl substituent at the imidazole ring. The observations of USCT were limited by the boiling temperature of the solvent. For [bmim][PF_6] the rapid change of the solubility was observed for the mole fractions $x_1 = 0.34$ and $x_1 = 0.56$ in benzene and toluene, respectively, which suggests that USCTs are very high temperatures for these binary mixtures. It was impossible to detect by the visual method the mutual solubility of ILs in the solvent rich phase. The crystal disappearance even in a very diluted solution was possible to observe, but the observation of the liquid−liquid demixing was inhibited by the permanently foggy solution. Such an observation in the solvent rich region is possible for the [emim][PF_6] in alcohols.[26] The spectroscopic or other techniques are necessary in the mixtures under study. The existence of the liquid−liquid equilibria in these mixtures is the evidence that the interaction between the IL and the solvent is not significant. A hypothesis was advanced previously[27,28] that the dissolution of a self-associated solid substance in a nonpolar solvent consists of transferring the associates existing in the crystal phase into saturated solution. The types of hydrogen-bonded associates formed in phenol and aromatic acid crystals were discussed, as was their effect on solid−liquid equilibrium. The molecules in the crystal very often occur as more complex structures, such as ILs formed with the aid of the hydrogen bonds. Dissolution of such a crystal in a nonpolar solvent may be supposed to involve the transfer of lattice-borne multimers into the solution. Thus, the crystal structure of ILs is very important and is responsible for the phase diagrams in binary mixtures of hydrogen-bonded ILs with different hydrocarbons. To our knowledge, the structures of [emim][PF_6] and [bmim][PF_6] are not known. Only the unit cell of the [C_{12}-mim][PF_6] salt was described as having a spoon-shaped structure,[29] being a result of strong interaction between the nitrogens of the imidazole ring and the special order of the alkyl chain.

Table 5. Correlation of the Solubility Data, SLE, of the [emim][PF_6] (1) + a Hydrocarbon (2) Mixtures by Means of the UNIQUAC and NRTL Equations: Values of Parameters and Measures of Deviations

	parameters		deviations	
	UNIQUAC Δu_{12} Δu_{21}	NRTL[a] Δg_{12} Δg_{21}	UNIQUAC σ_T[b]	NRTL σ_T[b]
hydrocarbon	J·mol^{-1}	J·mol^{-1}	K	K
benzene	3901.26	2467.92	0.87	0.76
	−1695.60	184.08		
toluene	5792.44	4791.99	0.70	0.63
	−2726.61	−1105.12		
ethylbenzene	6339.26	5168.02	0.09	0.09
	−3110.76	−1424.67		
o-xylene	7486.06	6580.41	0.17	0.16
	−3833.90	−2758.16		
m-xylene	7381.67	4734.14	0.48	0.57
	−3458.78	66421.03		
p-xylene	8107.95	7306.40	0.20	0.21
	−3847.31	−2466.21		

[a] Calculated with the third nonrandomness parameter α = 0.8. [b] According to eq 3 in the text.

Literature Cited

(1) Holbrey, J. D.; Seddon, K. R. Ionic liquids. *Clean Prod. Process.* **1999**, *1*, 223−236.
(2) Marsh, K. N.; Deev, A.; Wu, A. C.-T.; Tran, E.; Klamt, A. Room-Temperature Ionic Liquids as Replacements for Conventional Solvents—A Review. *Kor. J. Chem. Eng.* **2002**, *19*, 357−362.
(3) Anthony, J. L.; Maginn, E. J.; Brennecke, J. F. Solution Thermodynamics of Imidazolium-Based Ionic Liqids and Water. *J. Phys. Chem. B* **2001**, *105*, 10942−10949.
(4) Wong, D. S. H.; Chen, J. P.; Chang, J. M.; Chou, C. H. Phase Equilibria of Water and Ionic Liquids [emim][PF_6] and [bmim][PF_6]. *Fluid Phase Equilib.* **2002**, *194−197*, 1089−1095.
(5) Ngo, H. L.; LeCompte, K.; Hargens, L.; McEwen, A. B. Thermal Properties of Imidazolium Ionic Liquids. *Thermochim. Acta* **2000**, *357−358*, 97−102.

(6) Aki, S. N. V. K.; Brennecke, J. F.; Samanta, A. How Polar are Room-temperature Ionic Liquids? *Chem. Commun*. **2001**, *5*, 413−414.
(7) Law, G.; Watson, P. R. Surface Orientation in Ionic Liquids. *Chem. Phys. Lett*. **2001**, *345*, 1−4.
(8) Domańska, U.; Kozłowska, M. K.; Rogalski, M. Solubilities, Partition Coefficients, Density, and Surface Tension for Imidazoles + Octanol or + Water or + *n*-Decane. *J. Chem. Eng. Data* **2002**, *47*, 456−466.
(9) Rogalski, M.; Domańska, U.; Czyrny, D.; Dyczko, D. Surface and Conductivity Properties of Imidazoles Solutions. *Chem. Phys*. **2002**, *285*, 355−370.
(10) Domańska, U.; Bogel-Łukasik, E.; Bogel-Łukasik, R. 1-Octanol/Water Partition Coefficients of 1-Alkyl-3-methyl-imidazolium Chloride. *Chem. Eur. J*., in press.
(11) Domańska, U.; Kozłowska, M. K.; Rogalski, M. Solubility of Imidazoles in Alcohols. *J. Chem. Eng. Data* **2002**, *47*, 8−16.
(12) Domańska, U.; Kozłowska, M. K. Solubility of Imidazoles in Ethers. *J. Chem. Eng. Data*, in press.
(13) Domańska, U.; Kozłowska, M. K. Solubility of Imidazoles in Ketones. *Fluid Phase Equilib*., in press.
(14) Domańska, U.; Bogel-Łukasik, E.; Bogel-Łukasik, R. Solubility of 1-Dodecyl-3-methylimidazolium Chloride in Alcohols (C_2−C_{12}). *J. Phys. Chem. B* **2003**, *107*, 1858−1863.
(15) Fuller, J.; Carlin, R. T.; De Long, H. C.; Haworth, D. Structure of 1-Ethyl-3-methylimidazolium Hexafluorophosphate: Model for Room Temperature Molten Salts. *J. Chem. Soc., Chem. Commun*. **1994**, *3*, 299−300.
(16) Wu, B.; Reddy, R. G.; Rogers, R. D. Novel Ionic Liquid Thermal Storage For Solar Thermal Electric Power Systems. *Proc. Solar Forum 2002 Solar Energy, The Power to Choose*, April 21−25, 2001, Washington, DC.
(17) Barton, A. F. M. *CRC Handbook of Solubility Parameter*; CRC Press: Boca Raton, FL, 1985; p 64.
(18) Koel, M. Physical and Chemical Properties of Ionic Liquids Based on The Dialkylimidazolium Cation. *Proc. Estonian Acad. Sci. Chem*. **2000**, *49*, 145−155.
(19) Branco, L. C.; Rosa, J. N.; Moura Ramos, J. J.; Afonso, C. A. M. Preparation and Characterization of New Room-Temperature Ionic Liquids. *Chem. Eur. J*. **2002**, *8*, 3671−3677.
(20) Magee, J. W.; Blokhin, A. V.; Kabo, G. J.; Paulechka, Y. U. Heat Capacity and Enthalpy of Fusion for 1-Butyl-3-methylimidazolium Hexafluorophosphate. 17th IUPAC Conference on Chemical Thermodynamics, 28.07−02.08.2002, Rostock, Germany, p 306.
(21) Abrams, D. S.; Prausnitz, J. M. Statistical Thermodynamics of Liquid Mixtures: a New Expression for the Excess Gibbs Energy of Partly or Completely Miscible Systems. *AIChE J*. **1975**, *21*, 116−128.
(22) Renon, H.; Prausnitz, J. M. Local Composition in Thermodynamic Excess Functions for Liquid Mixtures. *AIChE J*. **1968**, *14*, 135−144.
(23) Domańska, U. Solubility of *n*-Alkanes (C_{16}, C_{18}, C_{20}) in Binary Solvent Mixtures. *Fluid Phase Equilib*. **1989**, *46*, 223.
(24) Vera, J. H.; Sayegh, G. S.; Ratcliff, G. A. A. Quasi Lattice Local Composition Model for the Excess Gibbs Free Energy of Liquid Mixtures. *Fluid Phase Equilib*. **1977**, *1*, 113−135.
(25) Hofman, T.; Nagata, I. Determination of Association Constants for Alcohols Based on Ethers as Homomorphs. *Fluid Phase Equilib*. **1986**, *25*, 113−128.
(26) Domańska, U.; Marciniak, A. Phase Diagrams of [emim][PF_6] in Alcohols. In preparation.
(27) Książczak, A. Solid−Liquid Equilibrium and the Hydrogen Bond in Crystals. *Fluid Phase Equilib*. **1983**, *15*, 1−9.
(28) Książczak, A. The Effect of Auto-Association on Solid−Liquid Equilibrium. *Fluid Phase Equilib*. **1986**, *28*, 39−56.
(29) Gordon, C. M.; Holbrey, J. D.; Kennedy, A. R.; Seddon, K. R. Ionic Liquid Crystals: Hexafluorophosphate Salts. *J. Mater. Chem*. **1998**, *8*, 2627−2636.

Received for review July 25, 2002. Accepted January 6, 2003.

JE020145G